Phytomedicine 52 (2019) 157–167

Contents lists available at ScienceDirect

Phytomedicine

journal homepage: www.elsevier.com/locate/phymed

Andrographis paniculata diterpenoids and ethanolic extract inhibit TNFα-induced ICAM-1 expression in EA.hy926 cells

Hung-Chih Lin[a,1], Chien-Chun Li[b,c,1], Ya-Chen Yang[d], Tzu-Hsuan Chiu[e], Kai-Li Liu[b,c], Chong-Kuei Lii[d,e,*], Haw-Wen Chen[e,*]

[a] *Division of Neonatology, College of Medicine and Department of Pediatrics, Children's Hospital of China Medical University and China Medical University Hospital, Taichung 404, Taiwan*
[b] *Department of Nutrition, Chung Shan Medical University, Taichung 402, Taiwan*
[c] *Department of Nutrition, Chung Shan Medical University Hospital, Taichung 402, Taiwan*
[d] *Department of Food Nutrition and Health Biotechnology, Asia University, Taichung 413, Taiwan*
[e] *Department of Nutrition, China Medical University, Taichung 404, Taiwan*

ARTICLE INFO

Keywords:
Andrographis paniculata
Andrographolide (AND)
14-Deoxy-11,12-didehydroandrographolide (deAND)
Intercellular adhesion molecule 1 (ICAM-1)
Nuclear factor-κB (NFκB)

ABSTRACT

Background: *Andrographis paniculata* (*A. paniculata*), a traditional herb in Southeastern Asia, is used to treat inflammation-mediated diseases. *Purpose:* The two major bioactive diterpenoids in *A. paniculata* are andrographolide (AND) and 14-deoxy-11,12-didehydroandrographolide (deAND). Because of the anti-inflammatory evidence for AND, we hypothesized that deAND might possess similar potency for inhibiting monocyte adhesion to the vascular endothelium, which is a critical event for atherosclerotic lesion formation.
Material: In the present study, we used 3-(4,5-dimethylthiazol-2-yl)-2,5-diphenyltetrazolium bromide (MTT) assay to determine cell viability. We evaluated the production of intracellular reactive oxygen species (ROS) by using DCFDA assay. We assayed the protein expression by using Western blot analysis, the mRNA expression by using RT-PCR, and the nuclear protein-DNA binding activity by using EMSA.
Results: We showed that pretreatment of EA.hy926 cells with *A. paniculata* ethanolic extract (APE), deAND, and AND significantly inhibited TNFα-induced ICAM-1 protein and mRNA expression, ICAM-1 promoter activity, and monocyte adhesion. TNFα-stimulated IKKβ phosphorylation, IκBα phosphorylation and degradation, p65 nuclear translocation, and NFκB nuclear protein-DNA binding activity were attenuated by pretreatment with APE, deAND, and AND. APE, deAND, and AND attenuated TNFα-induced Src phosphorylation and membrane translocation of the NOX subunits $p47^{phox}$ and $p67^{phox}$. Both APE and AND induced protein expression of heme oxygenase 1 and the glutamate cysteine ligase modifier subunit and enhanced glutathione content. Pretreatment with AND and deAND inhibited TNFα-induced ROS generation.
Conclusion: These results suggest that the mechanism by which APE, deAND, and AND down-regulates TNFα-induced ICAM-1 expression in EA.hy926 cells is via attenuation of activation of the IKK/IκB/NFκB pathway.

Introduction

Inflammation plays a critical role in the development of many chronic diseases, including atherosclerosis, type 2 diabetes, and Alzheimer disease (Tabas and Glass, 2013). Atherosclerosis is a major risk factor for cardiovascular disease (CVD), which is the leading cause of death and illness in developed countries (Pecoits-Filho et al., 2002). Atherosclerosis is characterized by the accumulation of lipids and leukocyte recruitment in the early stage of atheroma initiation (Libby et al., 2002). Cytokines such as TNFα, IL-2, and IFN-γ are

Abbreviations: AND, andrographolide; AP-1, activator protein 1; APE, A. paniculata ethanolic extract; BSO, buthionine sulphoximine; CVD, cardiovascular disease; deAND, 14-deoxy-11,12-didehydroandrographolide; DMEM, Dulbecco's modified Eagle's medium; ECs, endothelial cells; EMSA, electrophoretic mobility shift assay; FBS, fetal bovine serum; GCLC, glutamate cysteine ligase catalytic subunit; GCLM, glutamate cysteine ligase modifier subunit; GSH, glutathione; HO-1, heme oxygenase 1; ICAM-1, intercellular adhesion molecule 1; IκB, inhibitory kappa B; NAC, N-acetylcysteine; NFκB, nuclear factor-κB; NOX, NADPH oxidase; Nrf2, NF-E2-related factor-2; ROS, reactive oxygen species; VCAM-1, vascular cell adhesion molecule 1

* Corresponding authors.
E-mail addresses: cklii@mail.cmu.edu.tw (C.-K. Lii), chenhw@mail.cmu.edu.tw (H.-W. Chen).
[1] Authors contributed equally to this work.

https://doi.org/10.1016/j.phymed.2018.09.205
Received 29 January 2018; Received in revised form 3 August 2018; Accepted 17 September 2018

expressed in atherosclerotic lesions, particularly in association with the presence of a large number of monocytes and macrophages (Witztum and Lichtman, 2014).

TNFα is a pro-inflammatory cytokine that is produced by macrophages, endothelial cells (ECs), and smooth muscle cells of atherosclerotic arteries during inflammation (Barath et al., 1990). TNFα increases the adhesion of monocytes to ECs by inducing the expression of intercellular adhesion molecule 1 (ICAM-1) and vascular cell adhesion molecule 1 (VCAM-1) mediated by NFκB (Thorne et al., 1996).

Reactive oxygen species (ROS) are important messengers for inflammation and play a critical role in the pathogenesis of CVD, autoimmunity, and aging (Schieber and Chandel, 2014). TNFα triggers the generation of ROS. Excessive ROS activate signaling pathways that enhance the expression of other pro-inflammatory cytokines (Mitra and Abraham, 2006) and lead to vascular dysfunction (Sprague and Khalil, 2009). In ECs, the enzyme systems catalyzing ROS generation include NADPH oxidase (NOX), xanthine oxidase, NO synthase, mitochondrial respiration, lipoxygenase, and cyclooxygenase (Cai and Harrison, 2000). A previous study showed that activation of c-Src/NOX is involved in TNFα stimulation of ROS production and NFκB activation (Lee et al., 2009). c-Src is a member of the Src family of kinases which have long been recognized to regulate key cellular processes, including proliferation, survival, migration, and metastasis (Kim et al., 2009). In addition, Src was shown to mediate leukocyte/EC interactions at sites of inflammation by modulating adhesion molecule clustering on ECs (Tilghman and Hoover, 2002). Chowdhury et al. (2005) showed that c-Src mediates tyrosine phosphorylation of $p47^{phox}$ and regulates NOX activation in ECs exposed to hyperoxia. NOX is composed of the membrane-bound $gp91^{phox}$ and $p22^{phox}$, as well as the cytosolic subunits $p40^{phox}$, $p47^{phox}$, $p67^{phox}$, and Rac (Jiang et al., 2014). Activation of NOX is mediated by the phosphorylation of $p47^{phox}$ and $p67^{phox}$, which leads to membrane translocation and interaction with the membrane-bound subunits (Lu et al., 2014).

Glutathione (GSH), an important intracellular antioxidant, protects cells against oxidative stress and maintains redox homeostasis in cells (Rahman and MacNee, 1999). Glutamate cysteine ligase (GCL) is the rate-limiting enzyme for GSH synthesis and is composed of the glutamate cysteine ligase catalytic (GCLC) and modifier (GCLM) subunits (Lu, 2009). Knockout of the *Gclm* or *Gclc* gene decreases cellular GSH content in the aortas and liver (Chen et al., 2007; Weldy et al., 2012). Heme oxygenase 1 (HO-1) catalyzes the rate-limiting step in the oxidative degradation of heme and produces free iron, carbon monoxide, and biliverdin, which is further catabolized to bilirubin by biliverdin reductase (Gozzelino et al., 2010). HO-1 is believed to protect against various inflammatory diseases, because induction of HO-1 or administration of the end products of heme catabolism has a therapeutic effect in many inflammatory diseases. In our previous study, we showed that signaling molecules, such as PI3K/Akt, and transcription factors, such as NF-E2-related factor-2 (Nrf2) and activator protein 1 (AP-1), are involved in the regulation of HO-1 gene expression by andrographolide (AND, Fig. 1A), a labdane diterpenoid in *Andrographis paniculata* (Lu et al., 2014). Up-regulation of HO-1 is essential for inhibition of TNFα-induced ICAM-1 expression in ECs by AND (Yu et al., 2010).

A. paniculata (Burm.f.) Nees, a traditional herb in southern Asia, is used to treat colds, diabetes, fever, and diarrhea (Hossain et al., 2014). In addition, several lines of evidence indicate that *A. paniculata* has a broad range of pharmacological effects including anticancer (Chao et al., 2013), antihyperglycemic (Yu et al., 2003), anti-inflammatory (Yu et al., 2010), antioxidant (Lu et al., 2014), and immune-stimulatory (Calabrese et al., 2000). AND and 14-deoxy-11,12-didehydroandrographolide (deAND, Fig. 1B) are the first and second most abundant diterpenes in *A. paniculata* (Lim et al., 2012). In mice challenged with ovalbumin, AND and deAND can inhibit NFκB activation, which has the anti-inflammatory effect of reducing levels of IL-4, IL-5, and IL-13 in bronchoalveolar lavage fluid (Bao et al., 2009; Guan et al., 2011). In addition, AND suppresses TNFα-induced ICAM-1 expression and monocyte adhesion in ECs (Lu et al., 2014). On the other hand, deAND has been shown to effectively decrease the mortality rate and body weight loss in mice challenged with A/chicken/Hubei/327/2004 (H5N1) or A/PR/8/ 34 (H1N1) influenza A viruses (IAV) through anti-inflammatory and anti-IAV activities (Cai et al., 2016). The aim of this study was to investigate whether *A. paniculata* ethanolic extract (APE) and deAND have a similar anti-inflammatory effect on TNFα-induced ICAM-1 expression in EA.hy926 cells and the working mechanisms involved.

Materials and methods

Chemicals

Dulbecco's modified Eagle's medium (DMEM), RPMI-1640, RPMI-1640 without phenol red, penicillin/streptomycin solution, and 0.25% trypsin-EDTA were obtained from GIBCO (Grand Island, NY, USA). Fetal bovine serum (FBS) was purchased from HyClone (Logan, UT, USA). AND was purchased from Calbiochem (Darmstadt, Germany). Human TNFα, sodium bicarbonate, sodium pyruvate, HEPES, DMSO, buthionine sulphoximine (BSO), *N*-acetylcysteine (NAC), and 3-(4,5-dimethylthiazol-2-yl)-2,5-diphenyltetrazolium bromide (MTT) were purchased from Sigma-Aldrich (St. Louis, MO, USA). 2′,7′-Bis(2-carboxyethyl)-5(6)-carboxyfluorescein acetoxymethyl ester (BCECF-AM) was purchased from Molecular Probes (Eugene, OR, USA). TRIzol reagent and 2,7-dichlorofluorescin diacetate (H_2DCFDA) were purchased from Invitrogen (Carlsbad, CA, USA).

Cell culture

Cell culture was performed according to a procedure described by Lu and colleagues (2014). EA.hy926 cells were cultured in DMEM supplemented with 1.5 g/l $NaHCO_3$, 10% FBS, 100 U/ml penicillin, and 100 mg/ml streptomycin at 37 °C in a 5% CO_2 humidified incubator.

Preparation of 14-deoxy-11,12-didehydroandrographolide and A. paniculata ethanolic extract

We isolated and purified deAND and APE according to the method of Dr. C.C. Chen, Hungkuang University, Taichung, Taiwan. Dried *A. paniculata* was procured from Taichung, Taiwan. Powered plant materials were extracted with 95% ethanol (1:5, w/v) at room temperature. After filtration by using Whatman filter paper, the filtrate was collected and the residue was repeatedly extracted until the filtrate turned colorless. Filtrate was concentrated under reduced pressure to 200 ml, and 100 ml was freeze-dried for 72 h. This filtrate was termed APE. The remaining 100 ml concentrate was transferred to a separatory funnel and 2000 ml of ethyl acetate (EA)/H_2O (1:1, v/v) was added for further extraction, which was repeated three times. The EA layer was collected and was concentrated under reduced pressure to 500 ml. We added an equal volume of silica gel (70–230 mesh) powder to the concentrate and placed it in the dark fume hood for adsorption. After volatilizing the EA, the adsorbed silica gel was further used for isolation and purification of compounds. Adsorbed silica gel was added to the upper layer of the column being filled with un-adsorbed silica gel (70–230 mesh). n-Hexane (n-H)/EA (10:1), n-H/EA (5:1), n-H/EA (3:1), n-H/EA (1:1), n-H/EA (1:2), n-H/EA (1:5), EA, EA/methanol (10:1), and EA/methanol (5:1) were used to elute the column sequentially. Every 200 ml of eluent was collected as a fraction and was concentrated under reduced pressure to 10 ml. The composition of each fraction was identified by thin layer chromatography. The fraction containing deAND was placed in a fume hood to evaporate the solvent and the crystal of deAND was harvested. By LC-MS, the purity of deAND recovered after crystallization from the solvents was 98%. The yield of deAND was 5.45 mg/g dried *A. paniculata*.

Our APE preparation contained approximately 5.5% by weight AND

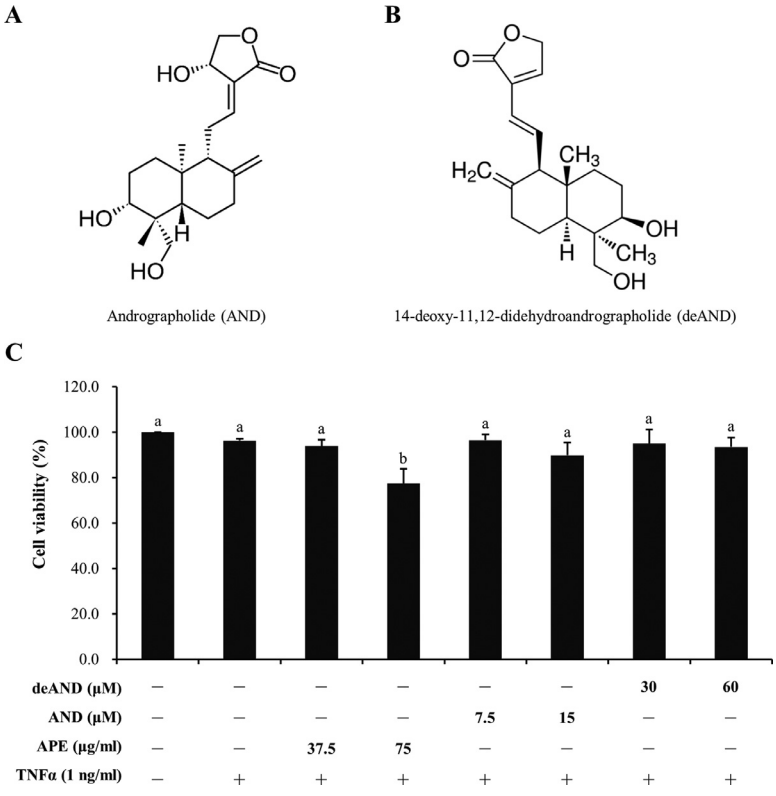

Fig. 1. Effects of *A. paniculata* ethanolic extract (APE), andrographolide (AND), and 14-deoxy-11,12-didehydroandrographolide (deAND) on cell viability of EA.hy926 cells in the presence of TNFα. Cells were pretreated with APE (37.5 and 75 μg/ml), AND (7.5 and 15 μM), or deAND (30 and 60 μM) for 16 h followed by incubation with 1 ng/ml TNFα for an additional 6 h. Cell viability was measured by using the MTT assay. Values are means ± SD of three independent experiments. Values not sharing the same letter are significantly different ($p < 0.05$).

and 2.5% by weight deAND. Therefore, 30 μg/ml APE used in this study contained about 4.69 μM AND and 2.25 μM deAND.

Cell viability assay

EA.hy926 cells were grown to 70% to 80% confluence and were then treated with different concentrations of APE (37.5 and 75 μg/ml), AND (7.5 and 15 μM), or deAND (30 and 60 μM) for 16 h followed by incubation with TNFα (1 ng/ml) for another 6 h. Thereafter, the cell viability assay was performed according to our previous study (Yu et al., 2010).

Subcellular fractionation

Subcellular fractionation was prepared as described by our previous study (Lu et al., 2014). Subcellular fractionation was obtained by use of the ProteoExtract Subcellular Proteome Extraction Kit (Calbiochem, Darmstadt, Germany).

Nuclear extract preparation

Nuclear extract preparation was performed as described by our previous study (Chao et al., 2011). Briefly, after each experiment, cells were washed twice with cold PBS and were then scraped from the dishes with 1 ml of PBS. Cell homogenates were centrifuged at 2000 x *g* for 5 min. The supernatant was discarded, and the cell pellet was allowed to swell on ice for 15 min after the addition of 200 μl of hypotonic buffer containing 10 mM HEPES, 1 mM $MgCl_2$, 1 mM EDTA, 10 mM KCl, 0.5 mM DTT, 0.5% Nonidet P-40, 4 μg/ml leupeptin, 20 μg/ml aprotinin, and 0.2 mM PMSF. After centrifugation at 7000 x *g* for 15 min, pellets containing crude nuclei were resuspended in 50 μl of hypertonic buffer containing 10 mM HEPES, 400 mM KCl, 1 mM $MgCl_2$, 0.25 mM EDTA, 0.5 mM DTT, 4 μg/ml leupeptin, 20 μg/ml aprotinin, 0.2 mM PMSF, and 10% glycerol at 4 °C for 30 min. The samples were then centrifuged at 20,000 x *g* for 15 min. The supernatant containing the nuclear proteins was collected and stored at −80 °C until electrophoretic mobility shift assay.

Western blot analysis

After each experiment, cells were washed twice with cold PBS and were harvested in 100 μl lysis buffer (10 mM Tris-HCl, pH 8.0, 0.1% Triton X-100, 320 mM sucrose, 5 mM EDTA, 1 mM PMSF, 1 μg/ml leupeptin, 1 μg/ml aprotinin, and 2 mM dithiothreitol). Cell homogenates were centrifuged at 10,000 x *g* for 20 min at 4 °C. The resulting supernatant was used as a cellular protein. The total protein was analyzed by use of the Coomassie Plus protein assay reagent kit (Thermo, Rockford, IL, USA). Equal amounts of cellular and nuclear proteins as well as the membrane fraction were electrophoresed in sodium dodecyl sulfate (SDS)-polyacrylamide gels, and proteins were then transferred to polyvinylidene difluoride membranes (Millipore, Billerica, MA, USA). Nonspecific binding sites on the membranes were blocked with 5% nonfat dry milk in 15 mM Tris/150 mM NaCl buffer (pH 7.4) at room temperature for 2 h. Membranes were probed with anti-IκBα and anti-GCLM (Santa Cruz Biotechnology, Santa Cruz, CA, USA); anti-ICAM-1, anti-phospho-IκBα (Ser32/36), anti-phospho-IKKα (Ser180)/IKKβ (Ser181), anti-PARP, anti-β-tubulin, anti-$p47^{phox}$, and anti-$p67^{phox}$ (Cell Signaling Technology, Boston, MA, USA); anti-GAPDH (Gene Tex, San Antonio, TX, USA); anti-GCLC (Abcam, Cambridge, UK); anti-HO-1 (Calbiochem, Darmstadt, Germany); antiphospho-Src (Invitrogen, Carlsbad, CA, USA); anti-p65 (BD Bioscience, San Jose, CA, USA); and anti-Na^+/K^+ ATPase (α1 subunit) (Millipore, Billerica, MA, USA) antibodies. The membranes were then probed with the secondary antibody labeled with horseradish peroxidase. The bands were visualized by using an enhanced chemiluminescence kit (Bio Kit, Miaoli, Taiwan) and were scanned by a luminescence image analyzer (Fuji Film LAS-4000, Tokyo, Japan). The bands were quantitated with Image-Gauge software (Fuji Film).

RNA isolation and reverse transcriptase polymerase chain reaction (RT-PCR)

Total RNA was extracted by using TRIzol reagent and frozen at −70 °C until RT-PCR analysis was performed. A total of 0.2 μg total RNA was used for the synthesis of first-strand cDNA by using Moloney murine leukemia virus reverse transcriptase (Promega Co., Madison, WI, USA) in a final volume of 20 μl containing 5 mM $MgCl_2$, 1 mM of each deoxynucleotide triphosphate, 2.5 mM of oligo-dT, and 40 U of RNase inhibitor. PCR was carried out in a thermocycler in a reaction volume of 50 μl containing 20 μl of cDNA, BioTaq PCR buffer, 4 mM $MgCl_2$, 1 U of BioTaq DNA polymerase (BioLine), and 6 pmol forward and reverse primers. Oligonucleotide primers were as follows: ICAM-1 (forward, 5′-ACCGTGTACTGGACTCCAGAA-3′; reverse, 5′-CGAGAAGG AGTCGTTGCCATA-3′) and GAPDH (forward, 5′-AGATCATCAGCAATG CCTCCT-3′; reverse, 5′-TCGTTGTCATACCAGGAAATGA-3′). Amplification of ICAM-1 and GAPDH was performed by heating samples to 94 °C for 5 min and then immediately cycling the samples 30 times through a 40-s denaturing step at 94 °C, a 40-s annealing step at 50 °C, and a 40-s elongation step at 72 °C. The GAPDH cDNA level was used as the internal standard. PCR products were resolved in a 1.5% agarose gel, scanned by a Digital Image Analyzer (Alpha Innotech), and quantitated with Image-Gauge software.

Electrophoretic mobility shift assay

Electrophoretic mobility shift assay (EMSA) was performed according to our previous study (Cheng et al., 2004). The Light-Shift Chemiluminescent EMSA Kit (Pierce Chemical Co., Rockford, IL, USA) and synthetic biotin-labeled double-stranded κB consensus oligonucleotides (forward: 5′-AGTTGAGGGGACTTTCCCAGGC-3′; reverse, 5′-GCCTGGGAAAGTCCCCTCAACT-3′) were used to measure NFκB nuclear protein-DNA binding activity. A total of 5 μg nuclear protein was used for the assay.

Reactive oxygen species measurement

Detection of intracellular oxidative states was performed by using the probe H_2DCFDA (Invitrogen, Carlsbad, CA, USA) as described previously (Yang et al., 2013). Briefly, cells were grown to 60%–70% confluence and were then serum-starved in DMEM supplemented with 0.5% (v/v) FBS for an additional 2 days. The cells were then stabilized in serum-free DMEM for at least 30 min before being challenged with TNFα. Thereafter, cells were incubated for 10 min with the ROS-sensitive fluorophore H_2DCFDA (10 μM) and were immediately observed under a laser-scanning confocal microscope (Leica TCS SP2). DCF fluorescence was excited at 488 nm with an argon laser and the evoked emission was filtered with a 515 nm long pass filter.

Cellular GSH measurement

The cellular GHS content was determined in cells treated with APE (30 μg/ml), AND (7.5 μM), or deAND (10 μM) as described previously (Lu et al., 2014). After each experiment, cells were washed twice with cold PBS and were harvested in 20 mM potassium phosphate buffer (pH 7.0). Cell homogenates were centrifuged at 10,000 x *g* for 20 min at 4 °C. The resulting supernatant was used as the cell lysate. The protein content of the cell lysate was measured by using the Coomassie Plus Protein Assay Reagent Kit. Afterwards, 150 ml of 5% TCA was added to 150 ml of cell lysates and centrifuged at 5000 x *g* for 10 min at 4 °C. The cell lysate was added to 0.4 M Tris buffer (with 0.02 M EDTA) and 0.01 M DTNB. After vortexing, the mixture was incubated at room temperature for 5 min, and the cellular GSH level was determined at 412 nm (Model 680 microplate reader, Bio-Rad).

Monocyte adhesion assay

Monocyte adhesion assay was performed according to a procedure described by Yu and colleagues (2010). Briefly, EA.hy926 cells challenged with TNFα for 6 h were incubated with BCECF-AM-labeled HL-60 cells at 37 °C for 30 min. Bound HL-60 cells were lysed in a 1% SDS solution, and the fluorescence intensity was determined in a fluoroscan ELISA plate reader (FLX800, Bio-Tek, Winooski, VT) with an excitation wavelength of 480 nm and an emission wavelength of 520 nm.

Plasmids, transfection, and luciferase assays

The ICAM-1 promoter-luciferase construct (pIC339, –339 to 0) was a gift from Dr. P.T. van der Saag (Hubrecht Laboratory, Utrecht, the Netherlands). pIC339 contains NFκB (–187/–178), AP-1 (–284/–279), AP-2 (–48/–41), and Sp1 (–59/–53, –206/–201) binding sites (van de Stolpe et al., 1994). The ICAM-1 promoter-luciferase activity was determined as described by Chao et al. (2011).

Statistical analysis

Data were analyzed by using analysis of variance (SAS Institute, Cary, NC, USA). The significance of the difference between mean values was determined by one-way analysis of variance followed by Tukey's test; p values <0.05 were taken to be statistically significant.

Results

Effects of APE, AND, and deAND on cell viability of EA.hy926 cells in the presence of TNFα

We used the MTT assay to test whether the concentrations of APE, AND, and deAND used in the presence of TNFα caused cell damage. As shown in Fig. 1C, APE (up to 37.5 μg/ml) had no adverse effects on the cell viability of EA.hy926 cells in the presence of 1 ng/ml TNFα, which was used to induce the expression of ICAM-1. AND (up to 15 μM) and deAND (up to 60 μM) also did not adversely affect the cell viability of EA.hy926 cells at the tested concentrations for 22 h. Thus, the effects of these compounds in the experiments were not due to their cytotoxicity.

APE, AND, and deAND inhibit TNFα-induced ICAM-1 expression and HL-60 adhesion

ICAM-1, an immunoglobulin (Ig)-like cell adhesion molecule, binds to integrin molecules such as LFA-1 and MAC-1 present on leukocytes and plays a critical role in the development of atherosclerotic lesions (Watanabe and Fan, 1998). *A. paniculata*, AND, and deAND have been shown to possess potent anti-inflammatory activity (Sheeja et al., 2006; Bao et al., 2009; Guan et al., 2011). In our previous studies, we showed that AND inhibits TNFα-induced ICAM-1 expression in a dose-dependent manner (Yu et al., 2010) and at least in part by attenuating the activation of NFκB in EA.hy926 cells (Chao et al., 2011). Here we studied whether APE and deAND possessed similar anti-inflammatory activity against TNFα-induced ICAM-1 expression. As shown in Fig. 2A, similar to AND found in our previous study (Yu et al., 2010), APE and deAND suppressed TNFα-induced ICAM-1 protein expression in a dose-dependent manner. Thereafter, we used 30 μg/ml APE, 7.5 μM AND, and 10 μM deAND for subsequent experiments (30 μg/ml APE contained approximately 4.69 μM AND and 2.25 μM deAND) because they showed a more potent inhibitory effect on TNFα-induced ICAM-1 expression under the tested doses; however, no adverse effect on cell viability was observed. As shown in Fig. 2B, APE, AND, and deAND significantly inhibited TNFα-induced ICAM-1 mRNA expression. As shown by ICAM-1 expression, AND had stronger anti-inflammatory activity than deAND.

The endothelial expression of adhesion molecules such as ICAM-1

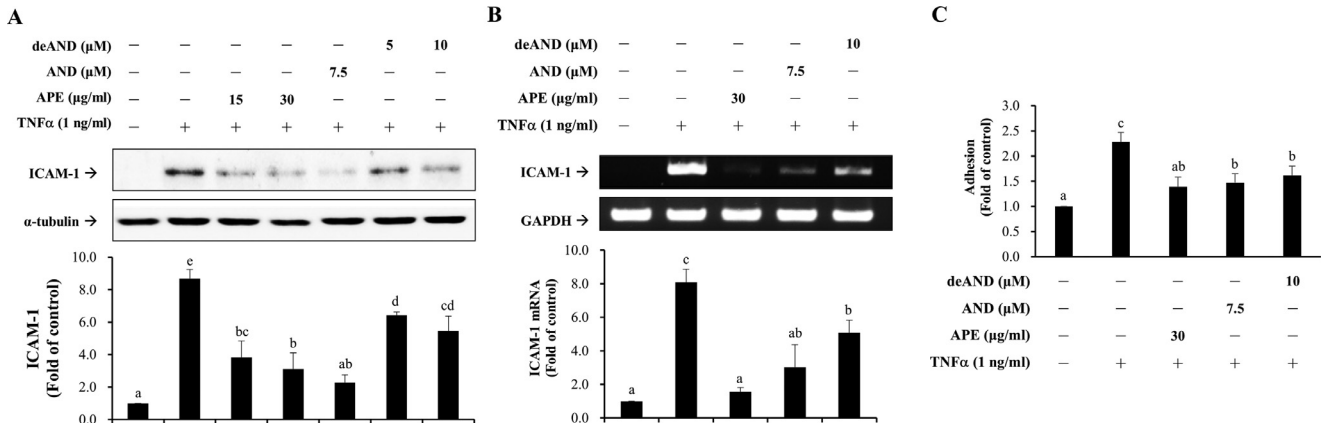

Fig. 2. *A. paniculata* ethanolic extract (APE), andrographolide (AND), and 14-deoxy-11,12-didehydroandrographolide (deAND) inhibit TNFα-induced ICAM-1 expression and HL-60 adhesion. (A) Cells were pretreated with 15 and 30 μg/ml APE, 7.5 μM AND, or 5 and 10 μM deAND for 16 h followed by incubation with 1 ng/ml TNFα for an additional 6 h. Aliquots of total protein (15 μg) were used for Western blot analysis. (B) Cells were pretreated with 30 μg/ml APE, 7.5 μM AND, or 10 μM deAND for 16 h followed by incubation with 1 ng/ml TNFα for an additional 4 h. Total RNA was isolated from cells and was subjected to RT-PCR with specific ICAM-1 and GAPDH primers as described in Materials and Methods. (C) Cells were pretreated with 30 μg/ml APE, 7.5 μM AND, or 10 μM deAND for 16 h before being challenged with 1 ng/ml TNFα for an additional 6 h. Cells were co-incubated with BCECF-AM-labeled HL-60 cells for 30 min, and then adhesion was determined as described in the Methods. Values are means ± SD of three independent experiments. Values not sharing the same letter are significantly different ($p < 0.05$).

contributes to monocyte recruitment in atherosclerosis (Thorne et al., 1996). Given that TNFα-induced ICAM-1 expression was inhibited by APE, AND, and deAND (Fig. 2A and 2B), we explored the effects of APE, AND, and deAND on TNFα-induced HL-60 adhesion. As shown in Fig. 2C, TNFα significantly induced HL-60 cell adhesion; however, this induction was attenuated by pretreatment with APE, AND, and deAND.

APE, AND, and deAND inhibit TNFα-induced activation of NFκB and promoter activity

The ICAM-1 promoter harbors several recognition sequences for transcription factors such as AP-1, AP-2, AP-3, NFκB, and Sp-1 (van de Stolpe et al., 1994). Among these, the NFκB binding site exhibits an important position with respect to TNFα-induced ICAM-1 expression. It is well recognized that activation of NFκB is mediated by IKK (Israël, 2010). Accordingly, we determined the effects of APE, AND, and deAND on the TNFα-induced IKK/IκBα/NFκB pathway. As shown in Fig. 3A, TNFα significantly induced IKKβ phosphorylation and this induction was abolished by pretreatment with APE, AND, and deAND. In addition to the activation of IKKβ, TNFα resulted in the phosphorylation and degradation of IκBα. The phosphorylation and degradation of IκBα induced by TNFα was mitigated by pretreatment with APE, AND, and deAND (Fig. 3A). Moreover, the effects of APE, AND, and deAND on TNFα-induced NFκB activation, in terms of nuclear accumulation of p65, were attenuated by pretreatment with APE, AND, and deAND (Fig. 3B). The EMSA results further corroborated that TNFα increased NFκB binding to the κB site in the ICAM-1 promoter and that pretreatment with APE, AND, and deAND attenuated NFκB nuclear protein-DNA binding activity (Fig. 3C). Thereafter, we investigated the role of APE, AND, and deAND in TNFα-induced ICAM-1 gene transcription. In these experiments, promoter activity was determined by using a human ICAM-1 promoter-luciferase construct, pIC339 (–339 to 0). APE, AND, and deAND inhibited TNFα-induced ICAM-1 promoter activity (Fig. 3D).

Effects of APE, AND, and deAND on TNFα-induced ROS generation in EA.hy926 cells

ROS are important mediators of inflammation, which is intimately associated with the development of chronic diseases (Tabas and Glass, 2013). Pro-inflammatory cytokines such as TNFα trigger the production of ROS, which not only results in endothelial dysfunction but also activates signaling pathways leading to the expression of other pro-inflammatory cytokines (Kim et al., 2007). Therefore, we tried to determine whether APE, AND, and deAND could inhibit TNFα-induced ROS generation. As shown in Fig. 4, TNFα induced ROS generation and pretreatment with AND and deAND significantly abrogated this induction. Unexpectedly, APE showed a synergistic effect with TNFα on ROS generation. tert-Butyl hydroperoxide (tBHP) was used as a positive control for ROS generation.

Effects of APE, AND, and deAND on TNFα-induced Src phosphorylation and NOX activation in EA.hy926 cells

A previous study showed that Src activation mediates TNFα-induced ICAM-1 phosphorylation, which is crucial for adhesion of polymononuclear leukocytes to the vascular endothelium (Liu et al., 2011). Activation of c-Src results in c-Src-dependent phosphorylation of $p47^{phox}$ and $p67^{phox}$, which leads to $p47^{phox}$ and $p67^{phox}$ membrane translocation and ROS production (Raad et al., 2009). As shown in Fig. 5, APE, AND, and deAND abolished TNFα-induced Src phosphorylation and membrane translocation of $p47^{phox}$ and $p67^{phox}$. Since Src phosphorylation is involved in NOX activation, the inhibition of TNFα-induced Src phosphorylation by AND and deAND is likely because they attenuate ROS generation. It is interesting to note that although APE inhibited TNFα-induced Src phosphorylation and membrane translocation of $p47^{phox}$ and $p67^{phox}$, APE did not suppress TNFα-induced ROS generation.

Effects of APE, AND, and deAND on cellular GSH content and the protein expression of antioxidant enzymes

GSH and GSH-related enzymes play a critical role in the maintenance of normal physiologic functions in humans. They are involved in the metabolism and detoxification of cytotoxic and carcinogenic compounds and in scavenging ROS (Knapen et al., 1999). Since APE, AND, and deAND all exhibited inhibitory effects on TNFα-induced monocyte adhesion (Fig. 2C), we studied their effects on cellular GSH contents. As shown in Fig. 6A, APE and AND but not deAND significantly increased the cellular GSH content. Concomitantly, we studied the effects of APE, AND, and deAND on the protein expression of antioxidant enzymes such as HO-1 and enzymes mediating GSH synthesis, including GCLC and GCLM. Both APE and AND significantly induced the protein expression of HO-1 and GCLM (Fig. 6B). In

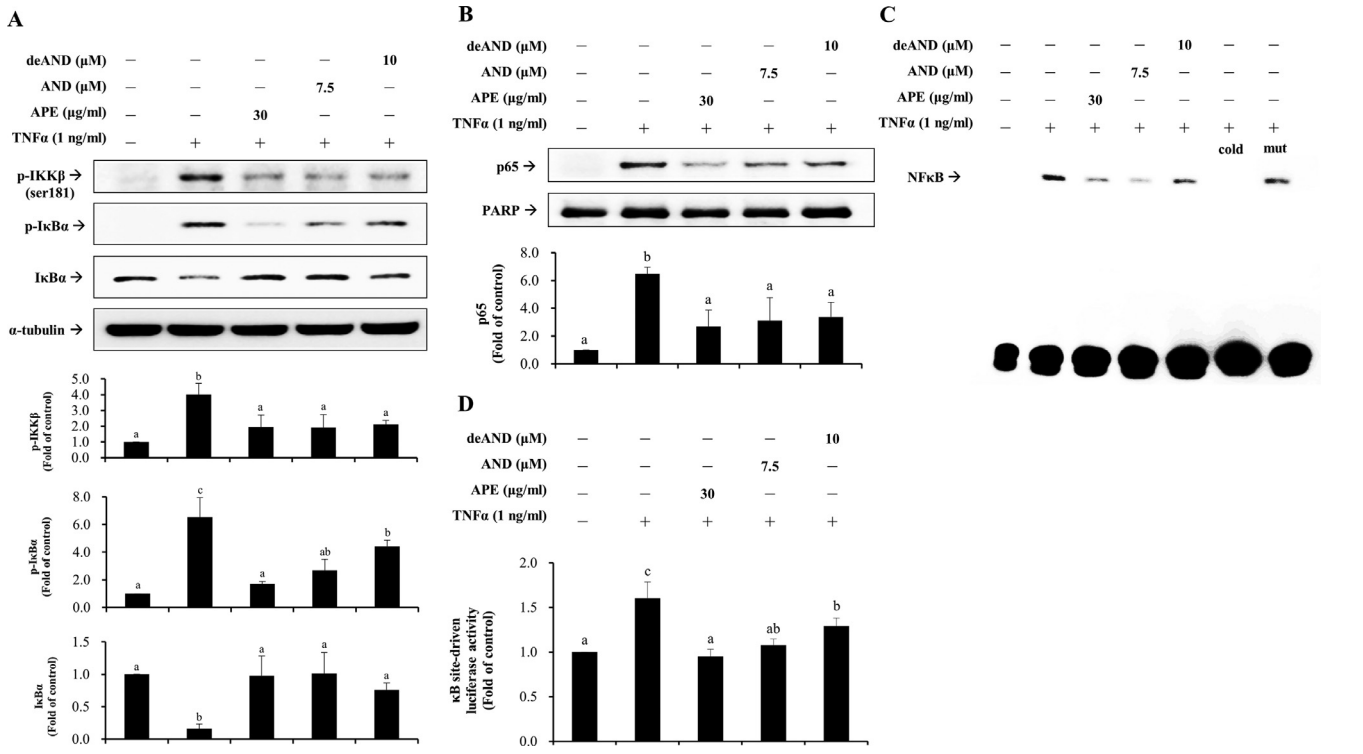

Fig. 3. *A. paniculata* ethanolic extract (APE), andrographolide (AND), and 14-deoxy-11,12-didehydroandrographolide (deAND) inhibit TNFα-induced activation of NFκB and promoter activity. (A) Cells were pretreated with 30 μg/ml APE, 7.5 μM AND, or 10 μM deAND for 16 h followed by incubation with 1 ng/ml TNFα for another 5 min. Aliquots of total protein (15 μg) were used for Western blot analysis. (B) Cells were pretreated with 30 μg/ml APE, 7.5 μM AND, or 10 μM deAND for 16 h followed by incubation with 1 ng/ml TNFα for an additional 2 h. Nuclear extracts (15 μg) were used for Western blot analysis. (C) Nuclear extracts (5 μg) were used for EMSA. (D) Cells transfected with the pIC339 luciferase expression vector were pretreated with 30 μg/ml APE, 7.5 μM AND, or 10 μM deAND for 16 h before being challenged with 1 ng/ml TNFα for an additional 6 h. Cells were then lysed and analyzed for luciferase activity. Induction was shown as an increase in the normalized luciferase activity in the treated cells relative to the control. Values are means ± SD of three independent experiments. Values not sharing the same letter are significantly different ($p < 0.05$).

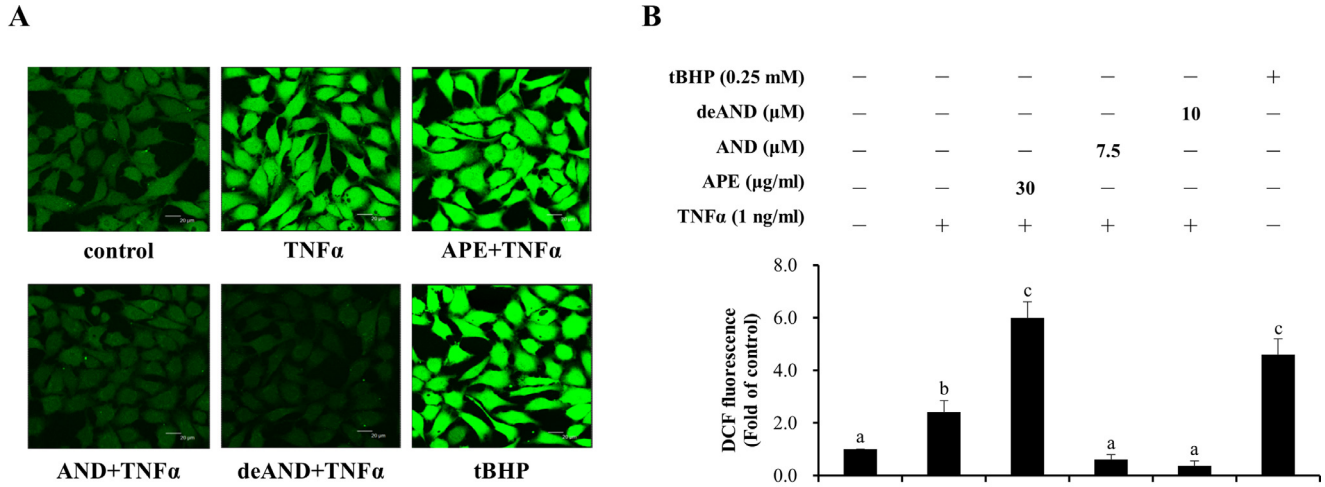

Fig. 4. Effect of *A. paniculata* ethanolic extract (APE), andrographolide (AND), and 14-deoxy-11,12-didehydroandrographolide (deAND) on TNFα-induced ROS generation in EA.hy926 cells. (A) Cells were stained with H_2DCFDA and visualized by fluorescence microscopy (scale bar = 20 μm). Cells were pretreated with 30 μg/ml APE, 7.5 μM AND, or 10 μM deAND for 16 h and incubated with 10 μM H_2DCFDA for 10 min before being challenged with 1 ng/ml TNFα for another 20 min. Stimulation with 0.25 mM tert-butyl hydroperoxide (tBHP) for 1 h was used as a positive control. Cells treated with 0.1% DMSO for 16 h were regarded as a vehicle control (CON). (B) Quantification of the ROS levels as detected by H_2DCFDA fluorescence intensities. Values are means ± SD of three independent experiments. Values not sharing the same letter are significantly different ($p < 0.05$).

contrast, deAND showed little effect on the protein expression of HO-1 and GCLM. These results suggested that the inhibition of TNFα-induced ROS generation by deAND was not associated with HO-1 expression or GSH synthesis.

Effect of GSH on AND inhibition of TNFα-induced ROS generation and IKKβ phosphorylation

Because AND induced GSH synthesis and GCLM protein expression (Fig. 6A and B), we therefore determined the role of GSH in the

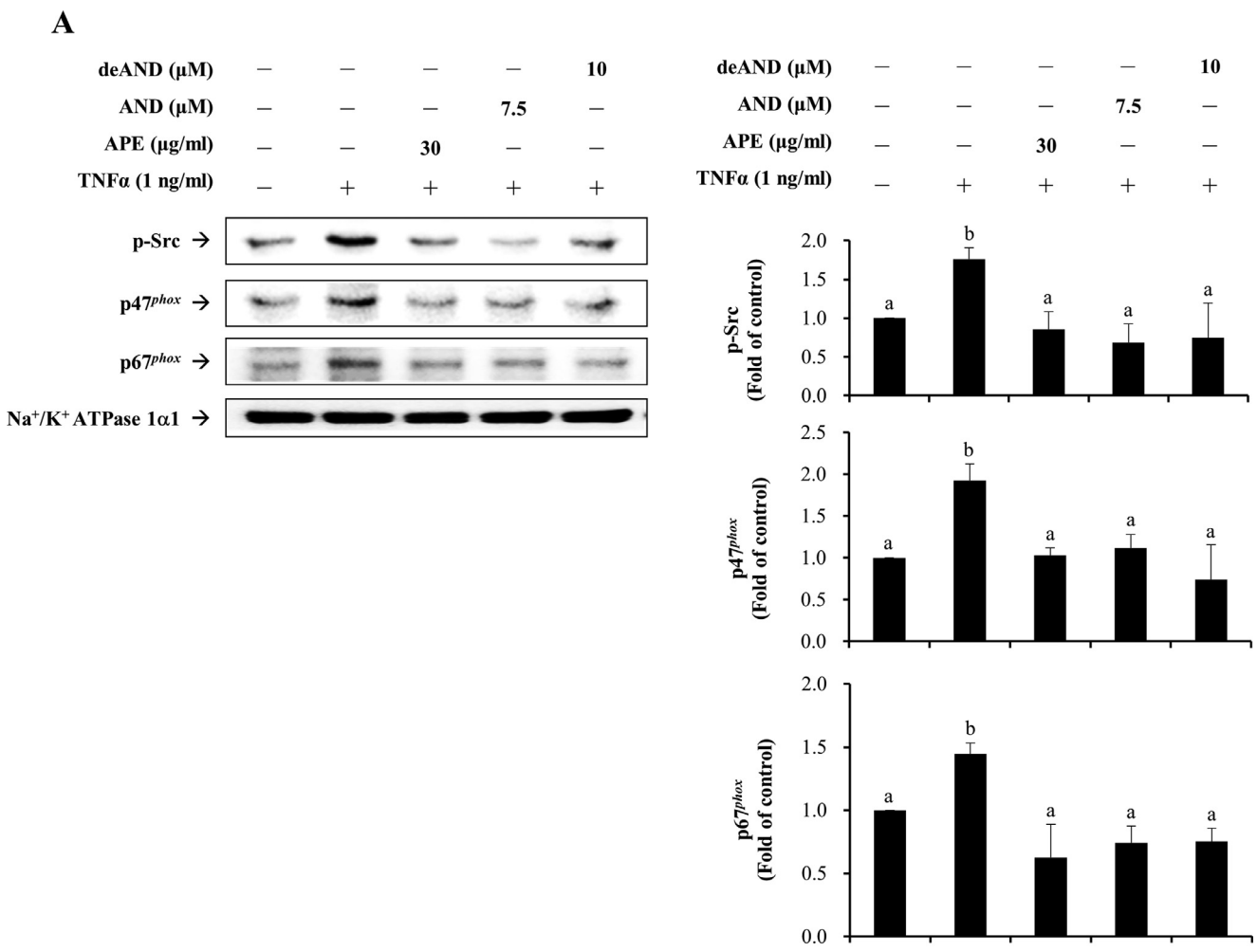

Fig. 5. Effects of *A. paniculata* ethanolic extract (APE), andrographolide (AND), and 14-deoxy-11,12-didehydroandrographolide (deAND) on TNFα-induced Src phosphorylation and NOX activation in EA.hy926 cells. Cells were pretreated with 30 μg/ml APE, 7.5 μM AND, or 10 μM deAND for 16 h followed by incubation with 1 ng/ml TNFα for another 1 h. Membrane fractions (15 μg) were used for Western blot analysis. Values are means ± SD of three independent experiments. Values not sharing the same letter are significantly different ($p < 0.05$).

inhibition of TNFα-induced ROS generation and IKKβ phosphorylation by AND. As shown in Fig. 7A, AND significantly increased GSH synthesis and BSO, a GSH synthesis inhibitor, suppressed AND-induced GSH synthesis. GSH is a well-known intracellular antioxidant and protects cells against oxidative stress (Rahman and MacNee, 1999). TNFα is a pro-inflammatory cytokine that induces ROS generation in EA.hy926 cells (Lu et al., 2014). In order to corroborate whether GSH is involved in the scavenging TNFα-induced ROS by AND, BSO treatment was performed. As shown in Fig. 7B, BSO treatment significantly abolished the suppression of TNFα-induced ROS by AND. In addition, we found that AND attenuated the TNFα-induced phosphorylation of IKKβ, whereas BSO treatment did not reverse this suppression (Fig. 7C). These results suggested that AND inhibited TNFα-induced ROS generation was GSH-dependent whereas AND suppressed TNFα-induced IKKβ phosphorylation was GSH-independent. Similar results regarding the role of GSH in TNFα-induced IKKβ activity were observed by Oka et al. (2000) who showed that TNF-induced IKKβ activity was inhibited by *N*-acetylcysteine (NAC) but this inhibition cannot be reversed by BSO although BSO suppressed NAC-stimulated GSH synthesis. NAC is a GSH precursor. Both we and Oka group indicated that inhibition of TNF-induced IKKβ activity was independent of cellular GSH.

Discussion

Oxidative stress is a manifestation of an imbalance between ROS production and disposal. Continued oxidative stress is associated with chronic inflammation, which in turn mediates several chronic diseases, including CVD, cancer, diabetes, neurological diseases, and pulmonary diseases (Reuter et al., 2010). Therefore, increased cellular antioxidant capacity is believed to protect against the development of diseases mediated by oxidative stress. APE contains over 20 diterpenoids and 10 flavonoids (Kishore et al., 2003; Li et al., 2007). The major labdanes in *A. paniculata* include AND and deAND. The maximum concentration of AND in blood was 0.35 μg/ml in rats intragastrically dosed with 50 mg/kg AND (Chen et al., 2014), and the maximum concentration of deAND in blood was 2.65 μg/mL in rats intragastrically dosed with 50 mg/kg deAND (unpublished data). In our previous studies, we showed that AND has antioxidant and anti-inflammatory activities via suppression of the TNFα-induced IKK/NFκB signaling pathway, NOX activation, and/or induction of HO-1 and GCLM expression (Yu et al., 2010; Chao et al., 2011; Lu et al., 2014). Compared with studies of the anti-inflammatory effects of AND, few studies have investigated the anti-inflammatory activity of deAND. One study reported that deAND has anti-inflammatory actions similar to AND in A549 and BEAS-2B human lung epithelial cells as well as rat basophilic leukemia (RBL)−2H3 cells (Guan et al., 2011). In addition to these in vitro data, deAND was shown to mitigate ovalbumin-induced airway eosinophilia, mucus production, mast cell degranulation, airway hyper-responsiveness, and the expression of the pro-inflammatory biomarkers IL-4, IL-5, and IL-13 in lung tissues (Guan et al., 2011). The anti-inflammatory activity of deAND is

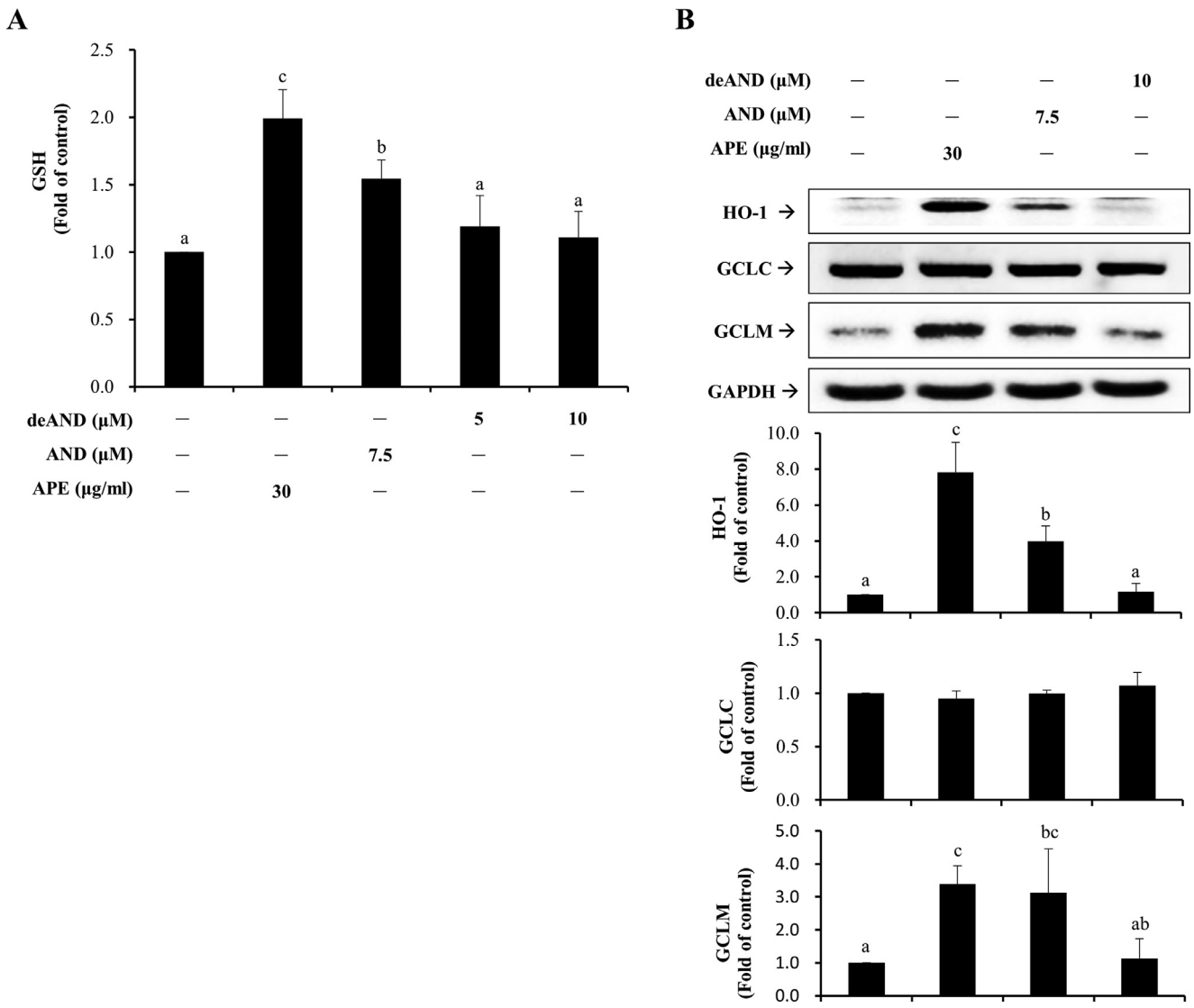

Fig. 6. Effects of *A. paniculata* ethanolic extract (APE), andrographolide (AND), and 14-deoxy-11,12-didehydroandrographolide (deAND) on cellular GSH content and antioxidant enzyme protein expression. (A) Cells were treated with 30 μg/ml APE, 7.5 μM AND, or 10 μM deAND for 24 h. Cell lysates were measured for GSH content. (B) The protein expression of heme oxygenase 1 (HO-1), GCLC, and GCLM was determined by Western blot analysis. Values are means ± SD of three independent experiments. Values not sharing the same letter are significantly different ($p < 0.05$).

ascribed to its inhibition of NFκB activation. In this study, we showed that APE, AND, and deAND all attenuated TNFα-induced ICAM-1 expression and monocyte adhesion and that this attenuation is likely associated with the suppression of NOX activation and the IKK/IκB/NFκB signaling pathway.

Atherosclerosis is a chronic inflammatory process that can result in an acute clinical event owing to plaque rupture, which in turn leads to thrombosis (Berliner et al., 1995). Atherosclerotic lesions are the consequence of inflammatory stimuli, the release of various cytokines, the proliferation of smooth muscle cells, and the accumulation of macrophages and lipids (Crowther, 2005). TNFα, a pro-inflammatory cytokine that triggers the inflammatory activation of ECs, is highly expressed in inflammatory diseases such as atherosclerosis and cancer (Kempe et al., 2005; Wu and Zhou, 2010). Activation of the transcription factor NFκB by TNFα is intimately associated with inflammation through increases in the expression of pro-inflammatory cytokines including IL-1 and MCP-1 as well as adhesion molecules like ICAM-1 (Collins et al., 1995; Thorne et al., 1996). TNFα has been shown to upregulate the expression of ICAM-1 through a TNFR1/TRAF2/PKCδ/JNK1/2-dependent c-Jun signaling pathway in retinal pigment epithelial cells (Lee et al., 2015). In addition, c-Src-driven IKK/NFκB activation takes part in TNFα-induced ICAM-1 expression in human lung epithelial A549 cells (Huang et al., 2003). Inhibition of NOX by apocynin and diphenyleneiodonium suppresses TNFα-induced ICAM-1 expression (Lu et al., 2014). NOX is one of the most important cellular sources of ROS, especially in blood vessels (Violi et al., 2009). In the present study, TNFα induced ROS generation (Fig. 4) in association with Src-mediated NOX activation (Fig. 5). The ability of AND and deAND to attenuate TNFα-induced ICAM-1 expression was through diminished Src phosphorylation, NOX activation, and ROS generation. However, the inhibitory effect of APE on TNFα-induced ICAM-1 expression could not be explained by the reduced ROS generation. Although APE abolished TNFα-induced Src phosphorylation and NOX activation, it augmented ROS generation by some unidentified mechanism, which suggests that NOX is not the source of ROS in the presence of APE. It has been shown that water extract of *A. paniculata* exhibits a prooxidant effect on GSH level in human erythrocytes (Cheunsombat et al., 2005). This supports our data that APE shows a prooxidant activity although AND and deAND have ROS-reducing activity. We cannot exclude that some unknown compounds present in

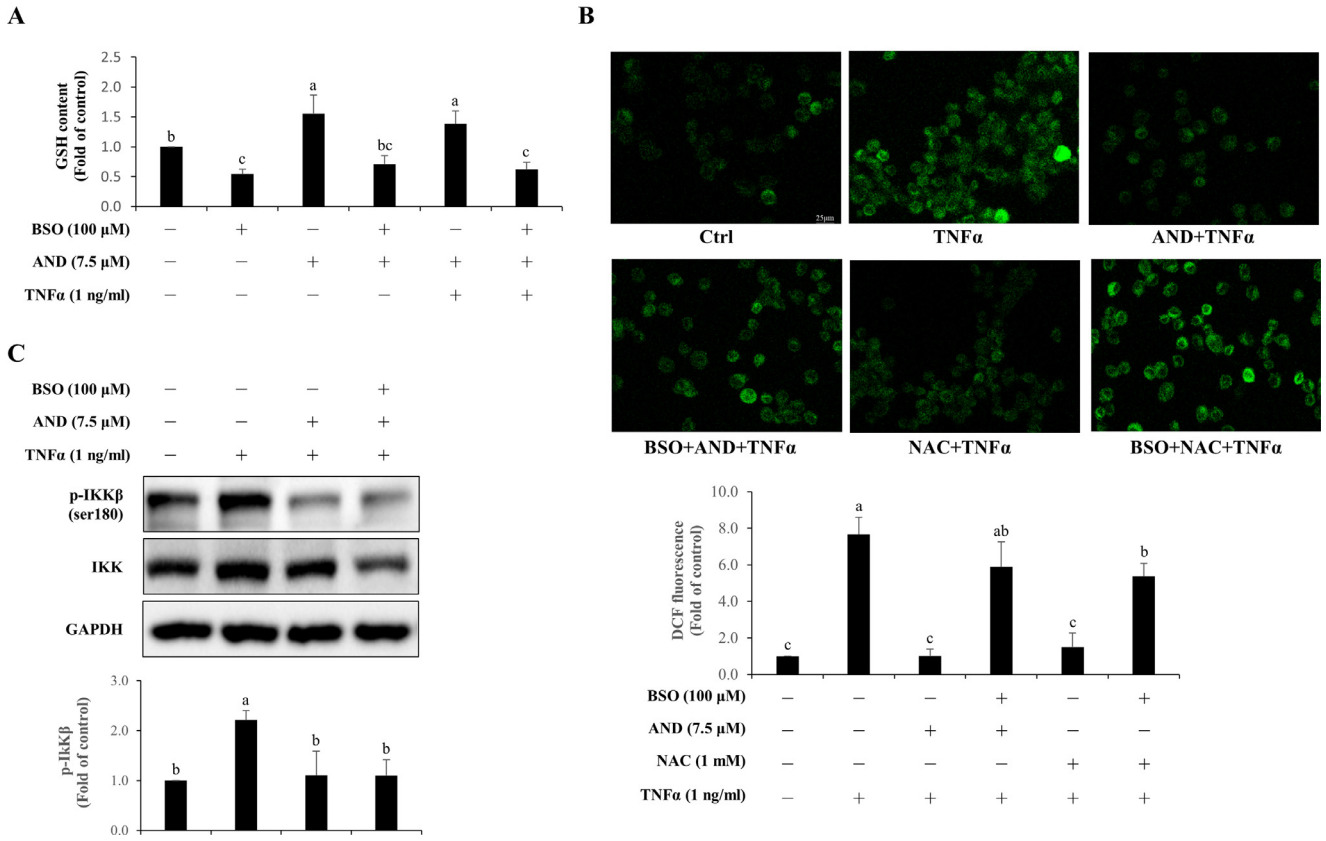

Fig. 7. Effect of GSH on andrographolide (AND) inhibition of TNFα-induced ROS generation and IKKβ phosphorylation. (A) Cells were treated with 7.5 μM AND in the presence or absence of 100 μM BSO for 16 h and then were stimulated with 1 ng/ml TNFα for additional 5 min. Cell lysates were measured for GSH content. (B) Cells were treated with 7.5 μM AND in the presence or absence of 100 μM BSO for 16 h or 1 mM NAC in the presence or absence of 100 μM BSO for 1 h and incubated with 10 μM H_2DCFDA for 10 min before being challenged with 1 ng/ml TNFα for another 20 min. Cells treated with 0.1% DMSO were regarded as a vehicle control (Ctrl). Quantification of the ROS levels as detected by H_2DCFDA fluorescence intensities. (C) Cells were treated with 7.5 μM AND in the presence or absence of 100 μM BSO for 16 h and then were stimulated with 1 ng/ml TNFα for additional 5 min. Aliquots of total protein (10 μg) were used for Western blot analysis. Values are means ± SD of three independent experiments. Values not sharing the same letter are significantly different ($p < 0.05$).

APE may trigger ROS generation. APE contains over 20 diterpenoids and 10 flavonoids (Kishore et al., 2003; Li et al., 2007). Since we just studied AND and deAND in the current study, there were still more diterpenoids and flavoids in APE unstudied which might possess prooxidant activity and show a synergistic effect with TNFα on ROS generation (Fig. 4A).

The important role of NFκB in the TNFα-induced expression of ICAM-1 and VCAM-1 has been demonstrated in human lung epithelial A549 cells (Oh et al., 2010). Furthermore, inhibition of NFκB by parthenolide has been shown to retard atherosclerotic lesions in apoE mice by reducing lesion size and changing plaque composition (López-Franco et al., 2006). As demonstrated in our previous study, TNFα phosphorylates IKKβ and IκBα (Yang et al., 2013). Phosphorylation of IκBα promotes its subsequent ubiquitination and proteasome degradation, which frees NFκB and facilitates its nuclear translocation. Our data indicated that APE, AND, and deAND all attenuated TNFα-induced phosphorylation of IKKβ and IκBα and reversed TNFα-induced degradation of IκBα (Fig. 3A). In addition, TNFα-induced nuclear accumulation of p65 was mitigated by treatment with APE, AND, and deAND (Fig. 3B). The activation of NFκB by TNFα was further supported by EMSA. TNFα-induced NFκB-DNA binding was attenuated by all three treatments (Fig. 3C). Moreover, TNFα induced κB-luciferase activity and this activity was mitigated by all three treatments as well (Fig. 3D). These results suggest that the IKK/IκB/NFκB signaling pathway is involved in the attenuation of TNFα-induced ICAM-1 expression by APE, AND, and deAND.

Antioxidants fight the adverse effects of radical reactions either directly or indirectly (Halliwell, 1995). GSH, a tripeptide, is an important cellular antioxidant. Its synthesis is regulated by GCL, which comprises the GCLC and GCLM subunits (Lu, 2009). In our previous study, we showed that AND can increase the cellular GSH content by activating GCLM (Lu et al., 2014). In the present study, we found that APE and AND rather than deAND significantly increased the cellular GSH content (Fig. 6A). Furthermore, we showed that the protein expression of GCLM was enhanced by APE and AND (Fig. 6B). AND stimulated GSH synthesis and this stimulation was abolished by BSO, a GSH synthesis inhibitor (Fig. 7A). In addition, BSO reversed the attenuation of TNFα-induced ROS generation by AND (Fig. 7B). In contrast, BSO did not affect the suppression of TNFα-induced IKKβ phosphorylation by AND (Fig. 7C). The results suggested that AND stimulated GSH synthesis, which scavenged TNFα-induced ROS generation. However, mitigation of TNFα-induced IKKβ phosphorylation by AND was independent of GSH. In addition to GSH, HO-1 is recognized to be a cytoprotective protein against oxidative stress (Turkseven et al., 2005). In the present study, APE and AND but not deAND induced protein expression of HO-1. The effect of AND on HO-1 expression is consistent with the results of our previous study (Lu et al., 2014). The induction of HO-1 expression by AND is mediated by the PI3K/Akt/Nrf2 and PI3K/Akt/AP-1 pathways.

Our findings in the current study are presented schematically in Fig. 8. The novelty of this study is the identification of deAND as an anti-inflammatory diterpenoid in APE. APE, deAND, and AND effectively down-regulate TNFα-induced ICAM-1 expression through different mechanisms in vascular ECs. Suppression of the IKK/IκB/NFκB signaling pathway is the common mechanism for APE, deAND, and AND to inhibit TNFα-induced ICAM-1 expression.

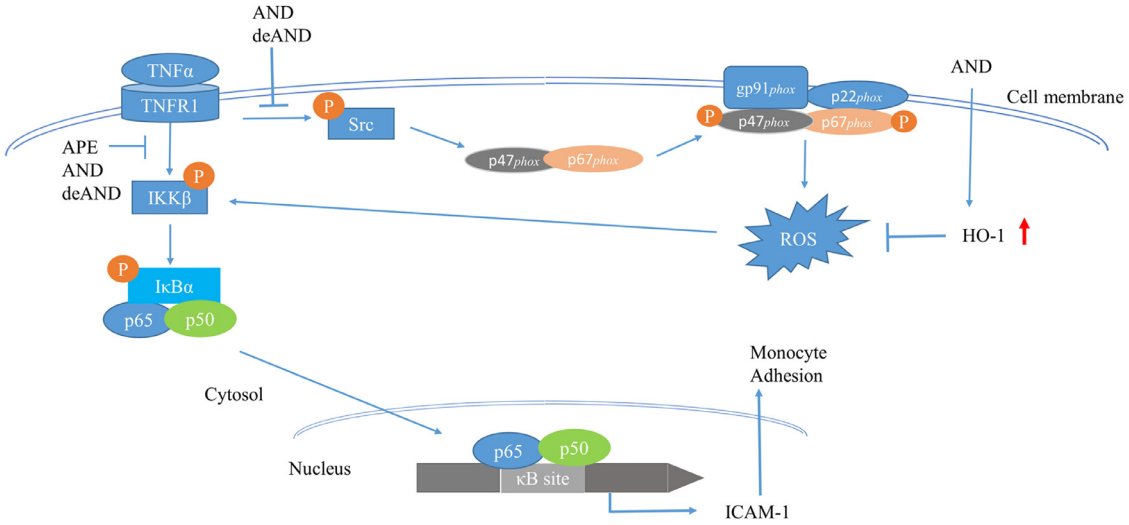

Fig. 8. Scheme summarizing the inhibition of TNFα-induced ICAM-1 expression by APE, AND, and deAND: APE, AND, and deAND reduce TNFα-induced IKK/IκB/NFκB pathway.

Conflict of interest

The authors have declared no conflict of interest.

Acknowledgments

This work was supported by grants CMU106-ASIA-09 and CMU107-ASIA-04 from China Medical University and Asia University, Taiwan.

References

Bao, Z., Guan, S., Cheng, C., Wu, S., Wong, S.H., Kemeny, D.M., Leung, B.P., Wong, W.S., 2009. A novel antiinflammatory role for andrographolide in asthma via inhibition of the nuclear factor-kappaB pathway. Am. J. Respir. Crit. Care Med. 179, 657–665.
Barath, P., Fishbein, M.C., Cao, J., Berenson, J., Helfant, R.H., Forrester, J.S., 1990. Tumor necrosis factor gene expression in human vascular intimal smooth muscle cells detected by in situ hybridization. Am. J. Pathol. 137, 503–509.
Berliner, J.A., Navab, M., Fogelman, A.M., Frank, J.S., Demer, L.L., Edwards, P.A., Watson, A.D., Lusis, A.J., 1995. Atherosclerosis: basic mechanisms oxidation, inflammation, and genetics. Circulation 91, 2488–2496.
Cai, H., Harrison, D.G., 2000. Endothelial dysfunction in cardiovascular diseases: the role of oxidant stress. Circ. Res. 87, 840–844.
Cai, W., Chen, S., Li, Y., Zhang, A., Zhou, H., Chen, H., Jin, M., 2016. 14-Deoxy-11,12-didehydroandrographolide attenuates excessive inflammatory responses and protects mice lethally challenged with highly pathogenic A(H5N1) influenza viruses. Antiviral Res. 133, 95–105.
Calabrese, C., Berman, S.H., Babish, J.G., Ma, X., Shinto, L., Dorr, M., Wells, K., Wenner, C.A., Standish, L.J., 2000. A phase I trial of andrographolide in HIV positive patients and normal volunteers. Phytother. Res. 14, 333–338.
Chao, C.Y., Lii, C.K., Hsu, Y.T., Lu, C.Y., Liu, K.L., Li, C.C., Chen, H.W., 2013. Induction of heme oxygenase-1 and inhibition of TPA-induced matrix metalloproteinase-9 expression by andrographolide in MCF-7 human breast cancer cells. Carcinogenesis 34, 1843–1851.
Chao, C.Y., Lii, C.K., Tsai, I.T., Li, C.C., Liu, K.L., Tsai, C.W., Chen, H.W., 2011. Andrographolide inhibits ICAM-1 expression and NF-κB activation in TNF-α-treated EA. hy926 cells. J. Agric. Food Chem. 59, 5263–5271.
Chen, H.W., Huang, C.S., Li, C.C., Lin, A.H., Huang, Y.J., Wang, T.S., Yao, H.T., Lii, C.K., 2014. Bioavailability of andrographolide and protection against carbon tetrachloride-induced oxidative damage in rats. Toxicol. Appl. Pharmacol. 280, 1–9.
Chen, Y., Yang, Y., Miller, M.L., Shen, D., Shertzer, H.G., Stringer, K.F., Wang, B., Schneider, S.N., Nebert, D.W., Dalton, T.P., 2007. Hepatocyte-specific Gclc deletion leads to rapid onset of steatosis with mitochondrial injury and liver failure. Hepatology 45, 1118–1128.
Cheng, W.L., Lii, C.K., Chen, H.W., Lin, T.H., Liu, K.L., 2004. Contribution of conjugated linoleic acid to the suppression of inflammatory responses through the regulation of the NF-κB pathway. J. Agric. Food Chem. 52, 71–78.
Cheunsombat, W., Banjerdpongchai, R., Rattanapanone, V., Punwong, D., 2005. Prooxidant effect of extract from Andrographis Paniculata Nees on glutathione levels in human erythrocytes. Chiang Mai Med. Bull. 44, 13–19.
Chowdhury, A.K., Watkins, T., Parinandi, N.L., Saatian, B., Kleinberg, M.E., Usatyuk, P.V., Natarajan, V., 2005. Src-mediated tyrosine phosphorylation of p47phox in hyperoxia-induced activation of NADPH oxidase and generation of reactive oxygen species in lung endothelial cells. .J. Biol. Chem. 280, 20700–20711.
Collins, T., Read, M.A., Neish, A.S., Whitley, M.Z., Thanos, D., Maniatis, T., 1995. Transcriptional regulation of endothelial cell adhesion molecules: NF-kappa B and cytokine-inducible enhancers. .FASEB J. 9, 899–909.
Crowther, M.A., 2005. Pathogenesis of atherosclerosis. Hematol. ASH Edu. Prog. 2005, 436–441.
Gozzelino, R., Jeney, V., Soares, M.P., 2010. Mechanisms of cell protection by heme oxygenase-1. Annu. Rev. Pharmacol. Toxicol. 50, 323–354.
Guan, S.P., Kong, L.R., Cheng, C., Lim, J.C., Wong, W.F., 2011. Protective role of 14-deoxy-11, 12-didehydroandrographolide, a noncytotoxic analogue of andrographolide, in allergic airway inflammation. J. Nat. Prod. 74, 1484–1490.
Halliwell, B., 1995. Antioxidant characterization. Methodology and mechanism. Biochem. Pharmacol. 49, 1341–1348.
Hossain, M.S., Urbi, Z., Sule, A., Rahman, K., 2014. Andrographis paniculata (Burm. f.) Wall. ex Nees: a review of ethnobotany, phytochemistry, and pharmacology. Sci. World J. 2014, 274905.
Huang, W.C., Chen, J.J., Chen, C.C., 2003. c-Src-dependent tyrosine phosphorylation of IKKbeta is involved in tumor necrosis factor-alpha-induced intercellular adhesion molecule-1 expression. J. Biol. Chem. 278, 9944–9952.
Israël, A., 2010. The IKK complex, a central regulator of NF-κB activation. Cold Spring Harb. Perspect. Biol. 2, a000158.
Jiang, F., Liu, G.S., Dusting, G.J., Chan, E.C., 2014. NADPH oxidase-dependent redox signaling in TGF-β-mediated fibrotic responses. Redox Biol. 2, 267–272.
Kempe, S., Kestler, H., Lasar, A., Wirth, T., 2005. NF-kappaB controls the global pro-inflammatory response in endothelial cells: evidence for the regulation of a pro-atherogenic program. Nucleic Acids Res. 33, 5308–5319.
Kim, M.P., Park, S.I., Kopetz, S., Gallick, G.E., 2009. Src family kinases as mediators of endothelial permeability: effects on inflammation and metastasis. Cell Tissue Res. 335, 249–259.
Kim, Y.S., Ahn, Y., Hong, M.H., Joo, S.Y., Kim, K.H., Sohn, I.S., Park, H.W., Hong, Y.J., Kim, J.H., Kim, W., 2007. Curcumin attenuates inflammatory responses of TNF-α-stimulated human endothelial cells. J. Cardiovasc. Pharmacol. 50, 41–49.
Kishore, P.H., Reddy, M.V., Reddy, M.K., Gunasekar, D., Caux, C., Bodo, B., 2003. Flavonoids from Andrographis lineata. Phytochemistry 63, 457–461.
Knapen, M.F., Zusterzeel, P.L., Peters, W.H., Steegers, E.A., 1999. Glutathione and glutathione-related enzymes in reproduction: a review. Eur. J. Obstet. Gynecol. Reprod. Biol. 82, 171–184.
Lee, I.T., Liu, S.W., Chi, P.L., Lin, C.C., Hsiao, L.D., Yang, C.M., 2015. TNF-alpha mediates PKCdelta/JNK1/2/c-Jun-dependent monocyte adhesion via ICAM-1 induction in human retinal pigment epithelial cells. PLoS One 10, e0117911.
Lee, I.T., Luo, S.F., Lee, C.W., Wang, S.W., Lin, C.C., Chang, C.C., Chen, Y.L., Chau, L.Y., Yang, C.M., 2009. Overexpression of HO-1 protects against TNF-α-mediated airway inflammation by down-regulation of TNFR1-dependent oxidative stress. Am. J. Pathol. 175, 519–532.
Li, J., Huang, W., Zhang, H., Wang, X., Zhou, H., 2007. Synthesis of andrographolide derivatives and their TNF-alpha and IL-6 expression inhibitory activities. Bioorg. Med. Chem. Lett. 17, 6891–6894.
Libby, P., Ridker, P.M., Maseri, A., 2002. Inflammation and atherosclerosis. Circulation 105, 1135–1143.
Lim, J.C.W., Chan, T.K., Ng, D.S., Sagineedu, S.R., Stanslas, J., Wong, W., 2012. Andrographolide and its analogues: versatile bioactive molecules for combating inflammation and cancer. Clin. Exp. Pharmacol. Physiol. 39, 300–310.
Liu, G., Vogel, S.M., Gao, X., Javaid, K., Hu, G., Danilov, S.M., Minshall, R.D., 2011. Src phosphorylation of endothelial cell surface ICAM-1 mediates neutrophil adhesion and contributes to the mechanism of lung inflammation. Arterioscler. Thromb. Vasc. Biol. 31, 1342–1350.
López-Franco, O., Hernández-Vargas, P., Ortiz-Muñoz, G., Sanjuán, G., Suzuki, Y., Ortega, L., Blanco, J., Egido, J., Gómez-Guerrero, C., 2006. Parthenolide modulates the NF-

kappaB-mediated inflammatory responses in experimental atherosclerosis. Arterioscler. Thromb. Vasc. Biol. 26, 1864–1870.
Lu, C.Y., Yang, Y.C., Li, C.C., Liu, K.L., Lii, C.K., Chen, H.W., 2014. Andrographolide inhibits TNFalpha-induced ICAM-1 expression via suppression of NADPH oxidase activation and induction of HO-1 and GCLM expression through the PI3K/Akt/Nrf2 and PI3K/Akt/AP-1 pathways in human endothelial cells. Biochem. Pharmacol. 91, 40–50.
Lu, S.C., 2009. Regulation of glutathione synthesis. Mol. Aspects Med. 30, 42–59.
Mitra, S., Abraham, E., 2006. Participation of superoxide in neutrophil activation and cytokine production. Biochimica et Biophysica Acta 1762, 732–741.
Oh, J.H., Park, E.J., Park, J.W., Lee, J., Lee, S.H., Kwon, T.K., 2010. A novel cyclin-dependent kinase inhibitor down-regulates tumor necrosis factor-alpha (TNF-alpha)-induced expression of cell adhesion molecules by inhibition of NF-kappaB activation in human pulmonary epithelial cells. Int. Immunopharmacol. 10, 572–579.
Oka, S., Kamata, H., Kamata, K., Yagisawa, H., Hirata, H., 2000. N-acetylcysteine suppresses TNF-induced NF-kappaB activation through inhibition of IkappaB kinases. FEBS Lett. 472, 196–202.
Pecoits-Filho, R., Lindholm, B., Stenvinkel, P., 2002. The malnutrition, inflammation, and atherosclerosis (MIA) syndrome–the heart of the matter. Nephrol. Dial. Transplant. 17, 28–31.
Raad, H., Paclet, M.H., Boussetta, T., Kroviarski, Y., Morel, F., Quinn, M.T., Gougerot-Pocidalo, M.A., Dang, P.M.C., El-Benna, J., 2009. Regulation of the phagocyte NADPH oxidase activity: phosphorylation of gp91phox/NOX2 by protein kinase C enhances its diaphorase activity and binding to Rac2, p67phox, and p47phox. FASEB J. 23, 1011–1022.
Rahman, I., MacNee, W., 1999. Lung glutathione and oxidative stress: implications in cigarette smoke-induced airway disease. Am. J. Physiol. 277 (6 Pt 1), L1067–L1088.
Reuter, S., Gupta, S.C., Chaturvedi, M.M., Aggarwal, B.B., 2010. Oxidative stress, inflammation, and cancer: how are they linked? Free Radical Biol. Med. 49, 1603–1616.
Schieber, M., Chandel, N.S., 2014. ROS function in redox signaling and oxidative stress. Curr. Biol. 24, R453–R462.
Sheeja, K., Shihab, P., Kuttan, G., 2006. Antioxidant and anti-inflammatory activities of the plant Andrographis paniculata Nees. Immunopharmacol. Immunotoxicol. 28, 129–140.
Sprague, A.H., Khalil, R.A., 2009. Inflammatory cytokines in vascular dysfunction and vascular disease. Biochem. Pharmacol. 78, 539–552.
Tabas, I., Glass, CK., 2013. Anti-inflammatory therapy in chronic disease: challenges and opportunities. Science 339, 166–172.
Thorne, S.A., Abbot, S.E., Stevens, C.R., Winyard, P.G., Mills, P.G., Blake, D.R., 1996. Modified low density lipoprotein and cytokines mediate monocyte adhesion to smooth muscle cells. Atherosclerosis 127, 167–176.
Tilghman, R.W., Hoover, R.L., 2002. The Src-cortactin pathway is required for clustering of E-selectin and ICAM-1 in endothelial cells. FASEB J. 16, 1257–1259.
Turkseven, S., Kruger, A., Mingone, C.J., Kaminski, P., Inaba, M., Rodella, L.F., Ikehara, S., Wolin, M.S., Abraham, N.G., 2005. Antioxidant mechanism of heme oxygenase-1 involves an increase in superoxide dismutase and catalase in experimental diabetes. Am. J. Physiol. Heart Circ. Physiol. 289, H701–H707.
van de Stolpe, A., Caldenhoven, E., Stade, B.G., Koenderman, L., Raaijmakers, J.A., Johnson, J.P., van der Saag, P.T., 1994. 12-O-tetradecanoylphorbol-13-acetate- and tumor necrosis factor alpha-mediated induction of intercellular adhesion molecule-1 is inhibited by dexamethasone. Functional analysis of the human intercellular adhesion molecular-1 promoter. J. Biol. Chem. 269, 6185–6192.
Violi, F., Basili, S., Nigro, C., Pignatelli, P., 2009. Role of NADPH oxidase in atherosclerosis. Future Cardiol. 5, 83–92.
Watanabe, T., Fan, J., 1998. Atherosclerosis and inflammation mononuclear cell recruitment and adhesion molecules with reference to the implication of ICAM-1/LFA-1 pathway in atherogenesis. Int. J. Cardiol. 66, S45–S53.
Weldy, C.S., Luttrell, I.P., White, C.C., Morgan-Stevenson, V., Bammler, T.K., Beyer, R.P., Afsharinejad, Z., Kim, F., Chitaley, K., Kavanagh, T.J., 2012. Glutathione (GSH) and the GSH synthesis gene Gclm modulate vascular reactivity in mice. Free Radical Biol. Med. 53, 1264–1278.
Witztum, J.L., Lichtman, A.H., 2014. The influence of innate and adaptive immune responses on atherosclerosis. Annu. Rev. Pathol. 9, 73–102.
Wu, Y., Zhou, B.P., 2010. TNF-alpha/NF-kappaB/Snail pathway in cancer cell migration and invasion. Br. J. Cancer 102, 639–644.
Yang, Y.C., Lii, C.K., Wei, Y.L., Li, C.C., Lu, C.Y., Liu, K.L., Chen, H.W., 2013. Docosahexaenoic acid inhibition of inflammation is partially via cross-talk between Nrf2/heme oxygenase 1 and IKK/NF-κB pathways. J. Nutr. Biochem. 24, 204–212.
Yu, A.L., Lu, C.Y., Wang, T.S., Tsai, C.W., Liu, K.L., Cheng, Y.P., Chang, H.C., Lii, C.K., Chen, H.W., 2010. Induction of heme oxygenase 1 and inhibition of tumor necrosis factor alpha-induced intercellular adhesion molecule expression by andrographolide in EA.hy926 cells. J. Agric. Food Chem. 58, 7641–7648.
Yu, B.C., Hung, C.R., Chen, W.C., Cheng, J.T., 2003. Antihyperglycemic effect of andrographolide in streptozotocin-induced diabetic rats. Planta Medica 69, 1075–1079.